Published in final edited form as:

Lab Chip. 2017 March 14; 17(6): 1051–1059. doi:10.1039/c6lc01167e.

A Low-Cost Smartphone-Based Platform for Highly Sensitive Point-of-Care Testing with Persistent Luminescent Phosphors

Andrew S. Paterson[†,Ψ], **Balakrishnan Raja**[†,Ψ], **Vinay Mandadi**[‡,Ψ], **Blane Townsend**[Ψ], **Miles Lee**[Ψ], **Alex Buell**[*], **Binh Vu**[†], **Jakoah Brgoch**[§], and **Richard C. Willson**[†,≠,||]

[†]Department of Chemical & Biomolecular Engineering, University of Houston

[Ψ]Luminostics, Inc., Houston, TX

[‡]Department of Mechanical Engineering, University of Houston

[*]Department of Computer Science, University of Houston

[§]Department of Chemistry, University of Houston

[≠]Department of Biology & Biochemistry, University of Houston

[||]Centro de Biotecnología FEMSA, Tecnológico de Monterrey, Campus Monterrey

Abstract

Through their computational power and connectivity, smartphones are poised to rapidly expand telemedicine and transform healthcare by enabling better personal health monitoring and rapid diagnostics. Recently, a variety of platforms have been developed to enable smartphone-based point-of-care testing using imaging-based readout with the smartphone camera as the detector. Fluorescent reporters have been shown to improve the sensitivity of assays over colorimetric labels, but fluorescence readout necessitates incorporating optical hardware into the detection system, adding to the cost and complexity of the device. Here we present a simple, low-cost smartphone-based detection platform for highly sensitive luminescence imaging readout of point-of-care tests run with persistent luminescent phosphors as reporters. The extremely bright and long-lived emission of persistent phosphors allows sensitive analyte detection with a smartphone by a facile time-gated imaging strategy. Phosphors are first briefly excited with the phone's camera flash, followed by switching off the flash, and subsequent imaging of phosphor luminescence with the camera. Using this approach, we demonstrate detection of human chorionic gonadotropin using a lateral flow assay and the smartphone platform with strontium aluminate nanoparticles as reporters, giving a detection limit of ≈45 pg/mL (1.2 pM) in buffer. Time-gated imaging on a smartphone can be readily adapted for sensitive and potentially quantitative testing

[*]Corresponding Author: willson@uh.edu.

Conflict of Interest Disclosure:

At the time this work was completed Andrew Paterson, Balakrishnan Raja, and Vinay Mandadi were employees of Luminostics, Inc., a company aiming to commercialize the smartphone platform discussed in this work and persistent luminescent phosphors as reporters. Blane Townsend and Miles Lee were contracted by Luminostics for smartphone app development. Andrew Paterson and Richard Willson are co-inventors on pending patents related to the present technology.

Supporting Information Available:

This material is available free of charge via the Internet at pubs.rsc.org.

using other point-of-care formats, and is workable with a variety of persistent luminescent materials.

Graphical Abstract

Time-gated imaging on a smartphone of a lateral flow test strip run with persistent luminescent nanophosphors.

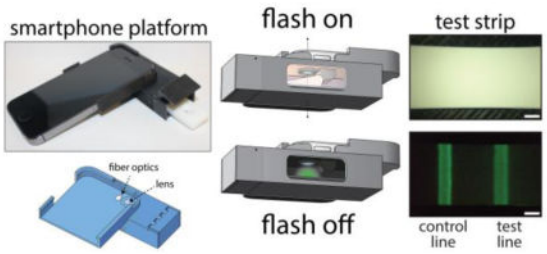

Keywords

persistent luminescence; phosphorescence; smartphone; diagnostics; nanoparticle; lateral flow assay; surface functionalization; time-gated detection; image analysis

Introduction

In recent years, a confluence of factors has ignited demand for highly sensitive point-of-care diagnostics. Healthcare providers need faster and more accurate diagnostic tools to improve patient outcomes and enhance workflow efficiency[1]. At the same time, a more technologically savvy populace has led to a surge in consumer health-related products such as smartphone apps and electronic devices for personal health monitoring and self-testing. Because smartphones have emerged as ubiquitous tools in modern society,[2] a natural approach to improving point-of-care testing is to enable smartphones to perform assay readout functionalities previously addressable only by specialized devices such as microplate readers[3] and optical[4] or fluorescence microscopes.[5,6]

One of the more promising strategies for enabling smartphone-based diagnostics is to integrate conventional point-of-care tests with the smartphone through an attachment that allows the phone's camera to function as a detector for imaging-based readout. Smartphone cameras have been used in point-of-care tests for both qualitative and quantitative detection of clinically relevant analytes such as small molecules including vitamin D[7] and cholesterol,[8] bacteria,[9] and numerous proteins and biomarkers.[10–12] Many of these smartphone-based platforms have been developed to work with the lateral flow assay (LFA),[11] a widely used point-of-care testing format which is the basis of the home pregnancy test[13] and the rapid HIV test.[14,15]

Conventional point-of-care testing formats such as LFAs, however, have struggled to achieve the low detection limits, high clinical sensitivities, and precise quantitation at low analyte levels necessary for accurate diagnosis in a variety of medical applications. This is due in

part to their frequent reliance on colorimetric labels such as submicron dyed latex particles and gold nanoparticles,[16] although sensitivity can be somewhat improved by using an automated reader instead of subjective visual interpretation. Sensitivity also can be improved by using fluorescence readout with some fluorescent reporters shown to give 10- to 100-fold improvements in detection limits over colorimetric labels.[17,18] In order to achieve a high signal-to-background ratio for sensitive fluorescence detection, however, the readout device must incorporate optical hardware such as excitation and emission filters or specialized light sources that increase cost and complexity. Additionally, some sample matrices and assay materials contain autofluorescent proteins or other molecules that emit at wavelengths overlapping the reporter emission,[19] creating a background that interferes with sensitive analyte detection.

An alternate approach to achieving high sensitivity comparable to fluorescence without relying on optical filters is to use time-gated detection.[20–22] Time-gated techniques rely on reporters that have relatively long emission lifetimes, typically on the order of $10–10^3$ μs, such as phosphorescent lanthanide chelate compounds.[23] A brief time-delay between excitation and measurement allows the background from scattered excitation light and autofluorescence to decay, enabling highly sensitive and specific detection of photoluminescence from the reporter with low background intensity. One of the main challenges with applying time-gated detection, however, is developing instrumentation that can precisely control such a short time delay, and rapidly and reproducibly initiate signal measurement after the delay with high temporal resolution. Early time-resolved microscopy systems relied on cumbersome and expensive mechanical chopper wheels or modulated lasers for time-gating,[19,23,24] but improvements in semiconductor device manufacturing led to simpler electronically-gated systems with superior synchronization and precision.[19] Solid-state lighting sources as such indium gallium nitride LEDs can be switched rapidly and extinguish quickly after being switched off, allowing them to be used in fluorescence lifetime measurements.[23,25] Additionally, both CMOS[26,27] and CCD[28] imaging sensors have been used for time-resolved detection with high temporal resolution.

In principle, current smartphones contain all the fundamental optical hardware necessary for time-gated imaging, with a rear camera that incorporates a CMOS image sensor and an InGaN-based LED as a light source in addition to a CPU for control. The next milestone in time-gated photoluminescence imaging is to extend this capability to smartphones for point-of-care testing. To our knowledge, there are no existing reports of the use of smartphones for time-gated imaging for analyte detection. This may be due in part to the proprietary nature of smartphone camera systems, which limits developers and researchers to working within the constraints of the application programming interfaces (APIs) provided by the manufacturer. Indeed, the inability to control exposure time and electronic gain, and a lack of access to the raw image format before post-processing, have been significant obstacles in developing robust cell phone microscopy systems.[29] Without access to the smartphone's camera and LED at the firmware level, controlling the time delay between excitation and imaging with microsecond temporal resolution, which is necessary for the more commonly used europium (Eu) chelate reporters, is very difficult. Furthermore, Eu-chelates generally have excitation spectral peaks in the deep UV[30], and thus, are not as effectively excited by a typical white LED package.

In contrast to short-lived fluorescent or phosphorescent molecules, a variety of crystalline inorganic phosphors have significantly longer emission lifetimes, exhibiting *persistent* luminescence that can be observed by eye for several hours after excitation.[31,32] The photoluminescence mechanism in persistent luminescent phosphors is distinct from the phosphorescence of organometallic compounds, which have longer emission lifetimes than typical fluorescent compounds due to the quantum mechanically forbidden process of intersystem crossing. In persistent luminescent inorganic materials, trap states present in the crystal structure capture charge carriers during photoexcitation. After excitation, thermal energy releases these charge carriers from the trap states where they are free to participate in photon emission processes at the luminescence center. The extraordinarily long-lived luminescence of persistent luminescent phosphors, and their ability to be excited by white light, has led to their widespread adoption in “glow-in-the-dark” products.[33,34] Their long emission lifetime gives persistent luminescent phosphors a unique advantage in analytical applications, by enabling sensitive time-gated readout without the constraint of short, precisely controlled microsecond time-delays.

We recently demonstrated that europium- and dysprosium-doped strontium aluminate ($SrAl_2O_4$: Eu^{2+}, Dy^{3+}) persistent luminescent nanophosphors gave better analytical sensitivity than gold nanoparticles in LFAs using a standard gel documentation reader equipped with a CCD camera for imaging-based readout.[35] However, the detection system described in that work is not ideally suited for point-of-care testing, due to the use of a cumbersome, relatively powerful UV lamp for excitation, and the high cost and size of the scientific camera used for luminescence imaging. Additionally, that system relied on manual control and timing of the excitation source and image acquisition trigger, which resulted in long, and variable time-delays. Furthermore, a long exposure time of ~6–8 min was previously used for image acquisition, which is impractical in many point-of-care testing applications.

Here we present a simple and compact smartphone-based platform for point-of-care testing which uses time-gated photoluminescence imaging as a highly sensitive and quantitative readout strategy for LFAs using persistent luminescent phosphor reporters. A software application controls the smartphone’s flash to excite the nanophosphors, after which the flash is turned off and the background light is allowed to decay (for *ca.* 100 msec) before the smartphone camera captures an image of the persistent luminescence from the reporters. We show that our time-gated imaging strategy with an iPhone 5s results in improved performance for sensitive analyte detection over the gel documentation reader system. This improvement was achieved despite the smartphone platform’s reliance on the phone’s built-in components, which provide a non-ideal excitation wavelength for the nanophosphor reporters and a CMOS image sensor expected to perform poorly compared to a scientific camera at detecting weak luminescence signals. We demonstrate the sensitivity of the smartphone platform by detection of human chorionic gonadotropin (hCG) in buffer in a lateral flow format, giving a detection limit of ≈45 pg/mL (1.2 pM), which is 10- to 100-fold more sensitive than many commercial LFAs and comparable in sensitivity to other photoluminescent readout methods. The smartphone platform can enable analyte quantitation, could be adapted to work with other point-of-care testing formats, and can

readily employ different types and colors of persistent luminescent phosphors for multiplexed detection.

Results and Discussion

Smartphone Attachment for Persistent Luminescence Lateral Flow Assay

A complete 3D-printed iPhone 5s attachment prototype is shown in Figure 1. The attachment is designed to slide easily onto a smartphone like a protective case, and contains a compartment that positions a lateral flow test cartridge in front of the camera and blocks out background light for sensitive luminescence imaging. When the test cartridge is fully inserted into the attachment, the test and control lines of the test strip align with the phone's rear camera and occupy most of the field of view (Supporting Information, Figure S-1). The attachment has no electronic components and minimal reliance on optical hardware, containing only a single plano-convex macro lens and a bundle of inexpensive plastic optical fibers in the simplest design. A concave parabolic reflective surface was later introduced to provide a more even illumination pattern for uniform excitation of phosphors within the field-of-view. When mass produced by methods widely used for low-cost plastic optics[36,37] such as injection molding and surface metallization by electroless plating for making plastic mirrors, the estimated cost of materials for the attachment is under ≈USD5. The low cost and simplicity of the design enables cheap, disposable smartphone attachments for diagnostics that can be discarded and recycled after a few uses if desired.

The lens serves several roles related to sensitivity and practicality. With the native optics, the iPhone 5s is unable to focus on objects within approximately ≈4 cm of the camera. The macro lens enables the camera to focus at a shorter distance, allowing a more compact and practical attachment design. With the reduced working distance, the lateral flow membrane sits closer to the camera and the flash, thereby enhancing nanophosphor excitation. The increased magnification and solid angle subtended by the lens also improves the detection of light emitted by the nanophosphors. It also gives a higher-resolution intensity profile of the test strip for more robust quantitative analysis. To further improve illumination of the sensing region and enhance excitation of the nanophosphors, the flash was redirected through a bundle of inexpensive plastic optical fibers. A plastic module bends the optical fibers such that light from the camera flash emerges at roughly a 55° angle with respect to the lateral flow strip. This design results in a slight asymmetry in the intensity profile of the light illuminating the membrane. To alleviate this asymmetry and produce a more even illumination of the sensing region, a concave, elliptical mirror was designed to surround the region containing the lens and fiber optics module (Figure S-3). The concave mirror further enhances excitation of the nanophosphors by confining light from the flash to the sensing region of the membrane and reducing scattering loss, although this is not essential for sensitive detection of nanophosphors.

Time-Gated Photoluminescence Imaging with a Smartphone

A schematic demonstrating time-gated imaging with the smartphone platform is shown in Figure 2. The cutaway view reveals the simplicity of the attachment, which is electrically inert and merely enhances the native optics of the camera phone with inexpensive

components, as both the detector (the phone's camera) and the excitation source (the phone's LED) are part of the phone. Smartphone based platforms designed for fluorescence imaging can require a number of components built into the attachment including excitation sources such as LEDs for specific fluorophores[16,38] and lasers for up-converting phosphors[39], batteries and electronics to power the excitation source, multiple lenses for both magnifying the image and collimating the excitation source, and optical filters. By implementing time-gated detection and leveraging the ultra-long emission property of persistent luminescence materials, one can eliminate the need for almost all of this hardware.

Time-Delay Control

In time-gated detection methods, one of the main factors affecting detection of the reporter is the time-delay between excitation and signal measurement. The luminescence intensity generally decays multi-exponentially, requiring that the detection system achieve prompt signal acquisition after excitation with high temporal resolution and reproducibility. Most time-gated assays use particles loaded with phosphorescent Eu-chelate compounds as reporters, with a typical time delay between excitation and measurement ranging from 10–500 μs.[21,22,30] While smartphone electronics may be fundamentally capable of time-gated imaging with time-delays in this range, iOS and Android APIs are limiting and currently do not provide sufficient tools for achieving such a precise level of control. We found that sub-millisecond time-delays were unattainable, indicating that time-gated detection on a smartphone would currently have poor performance with conventional Eu-chelate compounds.

We designed the time-gated imaging app to capture images with the smallest *reproducible* time-delay after excitation, during the bright initial decay of a persistent luminescent phosphor. The iPhone 5s LED can be controlled either in continuously-on "torch" mode, or in "flash" mode in which the LED outputs a bright burst of light for a brief period. The intensity of the LED is significantly higher in flash mode than torch mode (Supporting Information, Figure S-7), but the duration of the flash is short and cannot be altered. We found that turning on the LED in torch mode for 3 s, followed by triggering the flash, was the best option for both quick and effective excitation of the nanophosphors. A longer initial torch operation before the flash did not significantly improve detection of the phosphors.

Initial attempts to develop a script to command the smartphone's LED to turn on and off, followed by commands to capture an image, resulted in widely variable time delays from when the light turned off to the actual start of image acquisition, as determined from time-stamp data in log files generated when the app was executed. To achieve a consistent and short time delay, a different strategy, illustrated in the supporting information (Figure S-8), was used in which the camera captures continuous video at a high frame rate of 30 frames per second during excitation with the torch and flash. The captured frames are sampled to determine when the flash has turned off, and then the imaging settings are immediately changed to the maximum allowable exposure time and ISO setting for sensitive imaging of the persistent luminescence. The first frame in the series captured post-flash with the high sensitivity settings is saved as a high-resolution image for analysis. This time-gated imaging strategy resulted in a consistent time delay of approximately 100 ms. The total duration of

an imaging cycle when using a 3 s torch excitation followed by a flash, then image capture with a 0.5 s exposure time is currently about 5.3 s.

Noise Reduction

Historically, CMOS image sensors suffered from higher noise and poorer sensitivity than CCD sensors, particularly in low-light environments. This was due to a combination of factors including a low pixel fill factor inherent to older CMOS image sensor architectures, and noise from a variety of sources.[40] However, the low-light performance of CMOS image sensors has improved dramatically in recent years, driven largely by consumer demand for smartphones, with the introduction of technologies such as the back-illuminated CMOS sensors now used in most high-end smartphones.[41] Despite these significant advances, CMOS image sensors can still produce enough noise to be problematic when quantifying small signals in low-light conditions.

To dampen the effects of random noise, an image averaging approach was adopted in which multiple cycles of time-gated imaging are run with re-excitation by the camera torch and flash between each image. The resulting set of images is averaged together to form a composite image with significantly decreased noise.[42] The short excitation/imaging cycle time allows the execution of approximately 10 cycles per minute, so the signal-to-noise ratio can be improved through image averaging without significantly increasing the total time-to-result for the assay. A similar image stacking method has been shown to reduce noise and greatly enhance the detection of fluorescent dyes when using a CMOS webcam as the fluorescence detector.[43]

On a macroscopic scale, an ideal lateral flow test strip is spatially uniform across the width of the membrane, except for spotting variations in the test line and control line, and regions near the strip edges where the liquid flow rate differs from the bulk capillary flow rate in the membrane. This relative homogeneity was leveraged to calculate an average intensity profile down the length of the strip for quantitative analysis of the test and control lines. This “line scan averaging” method is illustrated in Figure 3, which shows the average intensity profile down the length of the strip as a function of the number of pixel columns averaged (≈1000 pixel columns for a 4 mm wide test strip) from the cropped image of the test strip. Line scan averaging results in an intensity profile with relatively low noise for robust quantitative analysis of the test line and control line intensities. An essential component in successfully implementing line scan averaging and automating image analysis of the lateral flow strip is precise location of the strip edges in the image. Details of the algorithm we developed to automatically locate strip edges are provided in the Supporting Information (Figure S-4).

Quantitative Image Analysis

Strategies for quantitative analysis of images include averaging the pixel intensity from a region of interest, and integration of intensity profiles. The selection of appropriate integration bounds, however, can be complicated by background variations. Alternately, extracting a quantitative assay readout metric from pixels inside pre-selected regions of interest such as the test and control lines appears to be a relatively straightforward method for analyte quantitation. Nonetheless, without careful selection of the box size and a

consistent algorithm for determining the box coordinates, this approach can introduce variability due to small variations in the width and position of the lateral flow test strip and lines.

We found that a robust strategy for analyzing the test strips is to first precisely determine the positions of the test line and control line by analyzing the intensity profile, and then to calculate the average pixel intensity within the test line and control line regions. This method is illustrated in Figure 4, which shows an image cropped at the strip edges and the corresponding line scan-averaged intensity profile below. A 1-D Gaussian smoothing operation is applied to the intensity profile, and the derivatives of the smoothed profile are used to find minima, maxima, and all inflection points in the profile. The inflection points of steepest slope correspond to the edges of the control line and test line, and the pixel intensities within the enclosed regions are averaged to give the effective intensity for the test line and control line. Only green pixels of the RGB image were used in these calculations because $SrAl_2O_4:Eu^{2+},Dy^{3+}$ has a green emission peak at 520 nm that most strongly overlaps with the green channel.

Lateral Flow Assay for Human Chorionic Gonadotropin

A very common application of LFA is rapid pregnancy testing by detecting human chorionic gonadotropin (hCG) in urine. The well-documented sensitivities of commercial hCG tests, and the abundance of publications using hCG as a model analyte make it an ideal system for evaluating the smartphone platform and comparing it to other technologies. To assess the relative sensitivity of time-gated imaging on a smartphone as a readout strategy, a lateral flow test for hCG was developed using silica-encapsulated $SrAl_2O_4:Eu^{2+},Dy^{3+}$ nanophosphors as reporters. We previously showed that strontium aluminate nanoparticles could improve detection limits by an order of magnitude over conventional gold nanoparticles in lateral flow tests using images captured with a gel documentation camera.[35]

Nanophosphors were functionalized with monoclonal anti-hCG antibodies as described in Materials and Methods and used to detect hCG. Figure 5 shows a dose response curve from three dilution series of hCG from 4.55 ng/mL down to 0.02 ng/mL, with duplicates for analyte concentrations under 1 ng/mL. Intensity ratios (I_{TL}/I_{CL}) were calculated with the test line and control line intensities determined using the pixel averaging method discussed previously. A detection limit cutoff taken as the mean plus three times the standard deviation of the no-target controls, is shown. The mean of the 0.05 ng/mL sample falls slightly above this cutoff line. Linear interpolation between 0.02 ng/mL and 0.05 ng/mL suggests a detection limit around 45 pg/mL (1.2 pM). We also captured images of the lateral flow strips with the FluorChem gel imager used previously, and found that the smartphone platform slightly outperforms the FluorChem (Supporting Information, Figures S-9–11), despite the imager having a CCD camera with a longer exposure time and a 370 nm UV lamp better-suited for excitation of the $SrAl_2O_4:Eu^{2+},Dy^{3+}$ nanophosphors. The short time-delay between excitation and imaging is a key factor in the performance of the smartphone system.

The analytical sensitivities of commercial lateral flow hCG tests vary, with most urine-based tests having detection limits around 25 IU/L (2.25 ng/mL or 61.4 pM according to the WHO 4th International Standard)[44], and the most sensitive tests having detection limits between 5–

10 IU/L (0.45–0.9 ng/mL).[44,45] Up-converting phosphors were reported to give a 0.1 ng/mL detection limit[46], and time-resolved immunofluorometric assays have been able to achieve detection limits down to 0.03 ng/mL.[47] The results in Figure 5 demonstrate that time-gated photoluminescence imaging with the smartphone platform and strontium aluminate nanophosphors can offer sensitivity comparable to or better than other light-based readout strategies, and sensitivity 10- to 50-fold better than commercial lateral flow tests.

The coefficients of variation for each analyte concentration are all under 15% and mostly less than 10%, indicating that the platform could be used for precise quantitation at low picomolar analyte concentrations. It should be noted that the mean of lowest concentration tested of ≈0.02 ng/mL is almost exactly two standard deviations away from mean of the no-target control. The detection limit of the platform could be readily pushed lower with additional optimization of the nanophosphor surface chemistry and wash buffer composition and better strip preparation to improve flow consistency. The detection limit also could be further improved by using brighter phosphors better optimized for use with the smartphone's platform, including better excitation spectral overlap with the 450 nm peak of the smartphone's LED. Brighter phosphors could enable using a lower ISO setting, which would result in images with lower noise, and therefore less variability in the test line and control line signals from random image sensor noise. Additionally, better smartphone hardware control to decrease the time-delay between excitation and imaging would increase the intensity of the signal from the nanophosphors which could also improve sensitivity.

Conclusions

We have developed a smartphone-based platform for sensitive readout of lateral flow tests using persistent luminescent phosphors as reporters. The platform can be used with any of the many inexpensive persistent phosphors that have significant excitation spectrum overlap with the emission of the phone flash, a luminescence emission peak at wavelengths detectable by the camera sensor, and a long enough luminescence lifetime to maintain a relatively high emission intensity for a few seconds after photoexcitation. The time-gated imaging strategy is able to achieve detection limits comparable to other photoluminescent reporters such as up-converting phosphors or fluorescent compounds, but with significantly simpler and less expensive readout hardware. The detection limit for hCG is 10-fold better than the best commercially available rapid pregnancy tests, and 50-fold better than the detection limit of the average commercial pregnancy test. Small coefficients of variation in the readout metric even at low analyte concentrations below 1 ng/mL indicate that the platform is a promising tool for point-of-care testing applications where precise quantitation at low analyte concentrations is essential.

Materials and Methods

Materials and Reagents

Tetraethyl orthosilicate (TEOS), (3-aminopropyl)triethoxysilane (APTES) 99%, bis[3-(trimethoxysilyl)propyl]amine (BTMOSPA) 96%, hydroxylamine hydrochloride, 3350 g/mol polyethylene glycol (PEG), Tween 20, bovine serum albumin (BSA), sodium periodate, 3-(N,N′dimethyloctadecylammonio)propanesulfonate (DOAPS-18)[48], N-

hydroxysuccinimide (NHS), sodium acetate, sodium chloride, HEPES sodium salt, and human chorionic gonadotropin (hCG) were purchased from Sigma-Aldrich. Sodium cyanoborohydride was purchased from Thermo Scientific. Ethyl acetate and 28–30% ammonium hydroxide were obtained from EM Science (Gibbstown, N.J.). Other reagents and their respective suppliers were glacial acetic acid (Macron), anhydrous ethanol (VWR), and phosphate buffered saline tablets (Bioline). Sodium hydroxide (Macron) and hydrochloric acid (Fisher Scientific) were used for titrating buffers to desired pH. Buffers were prepared with deionized water (Millipore Milli-Q) and filtered with nonpyrogenic sterile polystyrene filters (Corning Product # 430625). The strontium aluminate powder used to prepare the reporters used in all LFAs was purchased from Glow Inc. (Ultra Green v10 Glow in the Dark Powder).

3D Printing and Assembly of Smartphone Attachment

The components of the iPhone 5s attachment were designed using ViaCAD and Autodesk Inventor CAD software and 3D printed with a 5th Generation MakerBot and FlashForge Creator Pro desktop 3D printer. All parts were printed from black 1.75 mm diameter Hatchbox PLA filament or MakerBot True Black PLA. An exploded view of the attachment and the different 3D printed components is shown in Figure S-2 of the Supplementary Information along with additional details on the assembly process. The 3D printed parts were assembled using Loctite Ultra Gel Control Super Glue. The smartphone attachment was designed to hold a DCN Diagnostics (Carlsbad, CA) lateral flow test cartridge (Part Number MICA-125), with the result window of the cartridge aligned with the iPhone 5s rear camera and occupying most of the field of view when the cartridge is fully inserted into the attachment. A single 7 mm diameter plano convex lens with a 12 mm focal length (OptoSigma; Catalog # 011-0462-A55) was incorporated into the attachment. Approximately 280 individual 0.25 mm diameter plastic End Glow optical fibers (The Fiber Optic Store.com; Champlin, MN) were tightly packed into the fiber optics holder shown in Figure S-2. The holder bends the optical fibers such that light from the camera flash emerges at roughly a 55° angle with respect to the lateral flow strip. Once packed into the attachment, the optical fibers were cut to an approximate average length of ~0.6 cm. The end of the fiber optics bundle that contacts the phone was thoroughly sanded with silicon carbide sandpaper (Norton Abrasives; T414 Blue-Bak) to make a smooth flat surface that sits flush with the camera flash when the attachment is connected to the iPhone.

Image Processing and App Development

An iOS 9 software application (app) was written in Xcode for controlling the rear camera and flash of an iPhone 5s. The native autofocus algorithms were used to focus the smartphone camera on the membrane. With the macro lens in the attachment, the autofocus algorithms were found to focus consistently and quickly on the membrane. Time-delay control and image processing are described in detail in the Results and Discussion section. For the iPhone 5s used in the present work, the camera settings were ISO 2000 and a 0.5 s exposure time. The effectiveness of image averaging at improving the detection of phosphors was assessed using our own scripts that incorporate standard functions and image processing tools in MATLAB 2014b with image sets acquired using an iPhone 5s running the time-gated imaging app. All calculations for image processing described herein such as

image averaging, cropping, smoothing, derivation and integration, and intensity ratio calculations have been successfully implemented in the app and work directly on the iPhone 5s.

Preparation of Persistent Luminescent Nanophosphors

The nanophosphors were isolated from bulk materials following a wet milling and centrifugal size-fractionation process described previously.[35] The nanoparticles were then made water-stable by silica encapsulation. Typically, 1.0 mg of dry milled size-fractionated phosphors was suspended in 1 mL of anhydrous ethanol in a 2 mL microcentrifuge tube. A solution containing approximately 222 μL of ethanol, 247 μL of DI water, and 6.7 μL of TEOS was prepared, vigorously agitated, and then added immediately to the suspension of phosphors in ethanol. The tube with the particles was then placed in a bath sonicator (Fisher Scientific FS30) for 5 min, and afterward 25 μL of aqueous ammonium hydroxide (28–30%) was added to the reaction mixture, bringing the final volume to 1.5 mL. The calculated concentrations of TEOS and ammonia were 20 mM and 0.25 M respectively, with approximately 17.5% v/v water and 81.4% v/v ethanol. After adding the ammonium hydroxide, the particles were sonicated for an additional 30 min, and then placed on a room temperature rotator for 6.5 h to keep the particles suspended, with an overall silica encapsulation time of approximately 7 h. Silica encapsulation was stopped by centrifugal settling, removing the supernatant, and washing several times in ethanol.

Functionalization of Nanophosphors with anti-hCG Antibodies

Nanophosphors were functionalized with APTES to introduce primary amines for protein covalent coupling by dispersing ≈1 mg (dry strontium aluminate basis) of dried silica encapsulated phosphors in 920 μL of ethanol, then adding 50 μL of DI water, followed by 23.4 μL of APTES and 6.6 μL of BTMOSPA to make a 5:1 molar ratio of APTES to BTMOSPA. The suspension was placed in a batch sonicator for 20 minutes, then transferred to a room temperature rotator for an additional 40 minutes. After 1 hour since adding the APTES and BTMOSPA, the phosphors were taken off the rotator, centrifuged, and the supernatant was discarded. The phosphors were then washed 3 times in pure anhydrous ethanol, then dried for 3 hours under reduced pressure and elevated temperature (≈37°C) with the SpeedVac concentrator. Monoclonal mouse anti-β hCG antibodies (Arista Biologicals, Item # ABBCG-0402) were oxidized to introduce aldehydes[49,50] for coupling by first transferring the antibodies into pH 5.4 sodium acetate buffer with a 7k Zeba Spin Desalting Column (ThermoFisher, Catalog # 89882). A 100 mM stock solution of sodium periodate was prepared in sodium acetate buffer, then added to the buffer-exchanged antibodies so that the final sodium periodate concentration was 10 mM with an IgG concentration of ≈1 mg/mL. The oxidation reaction was carried out at room temperature for 1 hour, and then a second Zeba column was used to transfer the oxidized antibodies into PBS. Antibody coupling was then carried out by resuspending ≈1 mg (strontium aluminate dry basis) of the APTES-functionalized phosphors in PBS containing 0.1 mg/mL oxidized anti-β hCG antibodies and 250 mM sodium cyanoborohydride. The coupling reaction was allowed to proceed for 30 minutes at room temperature, and then ≈24 hours at 4°C on a rotator. The particles were quenched with 0.25 M hydroxylamine, passivated with 1 wt.% BSA, then washed and resuspended in PBS.

Nanophosphor hCG Lateral-Flow Assay

Whatman (GE Healthcare) FF80HP nitrocellulose membranes were used in all LFAs. Antibodies were spotted on the nitrocellulose membranes using a ClaremontBio Lateral Flow Reagent Dispenser powered by a programmable BK Precision 9130 DC power supply in combination with a Chemyx Inc. Fusion 200 syringe pump. Goat polyclonal anti-α hCG antibodies (Arista Biologicals, Item # ABACG-0500) were diluted from the stock concentration of 9.53 mg/mL to 1.2 mg/mL in DI water for the test line. The control line was prepared from a dilution of polyclonal goat anti-mouse IgG (Arista Biologicals, Item # ABGAM-0500) to 0.2 mg/mL in DI water from the 8.63 mg/mL stock concentration. The antibody solutions for the test line and control line were loaded into 1 mL BD Luer-Lok syringes, then connected to the syringe pump and dispensed at a rate of 0.2 mL/min with a 4 cm/s head speed. Membranes were dried for 30 min at 37°C in a Robbins Scientific Micro Hybridization Incubator 2000. The membranes were assembled on 0.010″ adhesive cards from DCN Diagnostics (Part # MIBA-020) with Whatman Standard 14 sample pads and Whatman CF7 absorbent pads. A ZQ2000 Guillotine Cutter from Diagnostic Tech Co. (Shanghai, China) was used to cut the strips to a 4 mm width.

The hCG LFAs were run using an assay buffer comprising pH = 7.5 50 mM HEPES buffer with 25 mM NaCl, 0.5 wt.% non-fat dry milk, 0.3 wt.% PEG-3350, 1 wt.% Tween-20, and 0.1 wt.% DOAPS-18. Dilutions of hCG into assay buffer were prepared, with no-target controls containing assay buffer with no hCG. For each strip, 50 μL of analyte in assay buffer was briefly mixed with 5 μL of 2 mg/mL anti-hCG phosphors, then the 55 μL volume was added to the strip. Washing was carried out with 80 μL of assay buffer.

Supplementary Material

Refer to Web version on PubMed Central for supplementary material.

Acknowledgments

This research was funded in parts by the NIAID/NIH (Grant No. U54 AI057156), the Huffington-Woestemeyer professorship, the University of Houston Technology Gap Fund (110412), NSF Innovation Corps Award (IIP-1450552). Development of the iPhone app was carried out in part with funding from Johns Hopkins University Applied Physics Laboratory (sub-contract 130521 via NIH U54EB007958). Its contents are solely the responsibility of the authors and do not necessarily represent the official views of the NSF, NIAID, NIH, or Johns Hopkins University.

References

1. Boppart SA, Richards-Kortum R. Sci Transl Med. 2014; 6:253rv252.
2. Erickson D, O'dell D, Jiang L, Oncescu V, Gumus A, Lee S, Mancuso M, Mehta S. Lab Chip. 2014; 14:3159–3164. [PubMed: 24700127]
3. Vashist SK, Van Oordt T, Schneider EM, Zengerle R, Von Stetten F, Luong JHT. Biosens Bioelectron. 2015; 67:248–255. [PubMed: 25168283]
4. D'ambrosio MV, Bakalar M, Bennuru S, Reber C, Skandarajah A, Nilsson L, Switz N, Kamgno J, Pion S, Boussinesq M, Nutman TB, Fletcher DA. Sci Transl Med. 2015; 7:286re284.
5. Zhu H, Yaglidere O, Su TW, Tseng D, Ozcan A. Lab Chip. 2011; 11:315–322. [PubMed: 21063582]
6. Breslauer DN, Maamari RN, Switz NA, Lam WA, Fletcher DA. PLoS One. 2009; 4:e6320. [PubMed: 19623251]

7. Lee S, Oncescu V, Mancuso M, Mehta S, Erickson D. Lab Chip. 2014; 14:1437–1442. [PubMed: 24569647]
8. Oncescu V, Mancuso M, Erickson D. Lab Chip. 2014; 14:759–763. [PubMed: 24336861]
9. Park TS, Li W, Mccracken KE, Yoon JY. Lab Chip. 2013; 13:4832–4840. [PubMed: 24162816]
10. Petryayeva E, Algar WR. RSC Adv. 2015; 5:22256–22282.
11. You DJ, Park TS, Yoon JY. Biosens Bioelectron. 2013; 40:180–185. [PubMed: 22863118]
12. Roda A, Guardigli M, Calabria D, Calabretta MM, Cevenini L, Michelini E. Analyst. 2014; 139:6494–6501. [PubMed: 25343380]
13. Posthuma-Trumpie GA, Korf J, Van Amerongen A. Anal Bioanal Chem. 2009; 393:569–582. [PubMed: 18696055]
14. Parisi MR, Soldini L, Di Perri G, Tiberi S, Lazzarin A, Lillo FB. New Microbiol. 2009; 32:391–396. [PubMed: 20128446]
15. Setty MKHG, Hewlett IK. AIDS Res Treat. 2014; 2014:1–20.
16. Lee LG, Nordman ES, Johnson MD, Oldham MF. Biosensors. 2013; 3:360–373. [PubMed: 25586412]
17. Zou Z, Du D, Wang J, Smith JN, Timchalk C, Li Y, Lin Y. Anal Chem. 2010; 82:5125–5133. [PubMed: 20507134]
18. Xia X, Xu Y, Zhao X, Li Q. Clin Chem. 2009; 55:179–182. [PubMed: 18974359]
19. Connally R, Veal D, Piper J. J Biomed Opt. 2004; 9:725–734. [PubMed: 15250759]
20. Song X, Knotts M. Anal Chim Acta. 2008; 626:186–192. [PubMed: 18790120]
21. Juntunen E, Myyryläinen T, Salminen T, Soukka T, Pettersson K. Anal Biochem. 2012; 428:31–38. [PubMed: 22705171]
22. Rundström G, Jonsson A, Mårtensson O, Mendel-Hartvig I, Venge P. Clin Chem. 2007; 53:342–348. [PubMed: 17185370]
23. Connally RE, Piper JA. Ann N Y Acad Sci. 2008; 1130:106–116. [PubMed: 18596339]
24. Marriott G, Clegg RM, Arndt-Jovin DJ, Jovin TM. Biophys J. 1991; 60:1374–1387. [PubMed: 1723311]
25. Connally R, Jin D, Piper J. Cytometry A. 2006; 69A:1020–1027.
26. Guo N, Cheung K, Wong HT, Ho D. Sensors. 2014; 14:20602–20619. [PubMed: 25365460]
27. Rae BR, Muir KR, Gong Z, Mckendry J, Girkin JM, Gu E, Renshaw D, Dawson MD, Henderson RK. Sensors. 2009; 9:9255–9274. [PubMed: 22291564]
28. Connally R, Piper J. J Biomed Opt. 2008; 13:034022. [PubMed: 18601567]
29. Skandarajah A, Reber CD, Switz NA, Fletcher DA. PLoS One. 2014; 9:e96906. [PubMed: 24824072]
30. Song X, Huang L, Wu B. Anal Chem. 2008; 80:5501–5507. [PubMed: 18510340]
31. Aitasalo T, Dereń P, Hölsä J, Jungner H, Krupa JC, Lastusaari M, Legendziewicz J, Niittykoski J, Stręk W. J Solid State Chem. 2003; 171:114–122.
32. Maldiney, T., Scherman, D., Richard, C. Functional Nanoparticles for Bioanalysis, Nanomedicine, and Bioelectronic Devices. Vol. 2. American Chemical Society; 2012. p. 1-25.
33. Botterman J, Smet PF. Optics Express. 2015; 23:A868. [PubMed: 26367687]
34. Van Den Eeckhout K, Smet PF, Poelman D. Materials. 2010; 3:2536–2566.
35. Paterson AS, Raja B, Garvey G, Kolhatkar A, Hagström AEV, Kourentzi K, Lee TR, Willson RC. Anal Chem. 2014; 86:9481–9488. [PubMed: 25247754]
36. Bäumer, S. Handbook of Plastic Optics. 2. Wiley-VCH; Weinheim: 2010.
37. Koike, Y. Fundamentals of Plastic Optical Fibers. Wiley-VCH; Weinheim: 2015.
38. Thom NK, Lewis GG, Yeung K, Phillips ST. RSC Adv. 2014; 4:1334–1340. [PubMed: 24490035]
39. Mei Q, Jing H, Li Y, Yisibashaer W, Chen J, Nan B. Biosens Bioelectron. 2016; 75:427–432. [PubMed: 26356763]
40. Bigas M, Cabruja E, Forest J, Salvi J. Microelectronics J. 2006; 37:433–451.
41. Fontaine, R. 2013 International Image Sensor Workshop. Snowbird Resort; Utah: 2013. p. 1-4.
42. Willson, R., Paterson, A. Phosphorescent reporters. US 14/461,118. 2015.

43. Balsam J, Bruck HA, Kostov Y, Rasooly A. Sens Actuators B Chem. 2012; 171–172:141–147.
44. Cole LA. Clin Chem Lab Med. 2011; 49:1317–1322. [PubMed: 21812725]
45. Cole LA, Sutton-Riley JM, Khanlian SA, Borkovskaya M, Rayburn BB, Rayburn WF. J Am Pharm Assoc. 2005; 45:608–615.
46. Hampl J, Hall M, Mufti NA, Yao YMM, Macqueen DB, Wright WH, Cooper DE. Anal Biochem. 2001; 288:176–187. [PubMed: 11152588]
47. Alfthan H, Haglund C, Dabek J, Stenman UH. Clin Chem. 1992; 38:1981–1987. [PubMed: 1382894]
48. Castelletti L, Verzola B, Gelfi C, Stoyanov A, Righetti PG. J Chromatogr A. 2000; 894:281–289. [PubMed: 11100871]
49. Raja B, Pascente C, Knoop J, Shakarisaz D, Sherlock T, Kemper S, Kourentzi K, Renzi RF, Hatch AV, Olano J, Peng BH, Ruchhoeft P, Willson R. Lab Chip. 2016; 16:1625–1635. [PubMed: 27025227]
50. Kang JH, Choi HJ, Hwang SY, Han SH, Jeon JY, Lee EK. J Chromatogr A. 2007; 1161:9–14. [PubMed: 17543979]

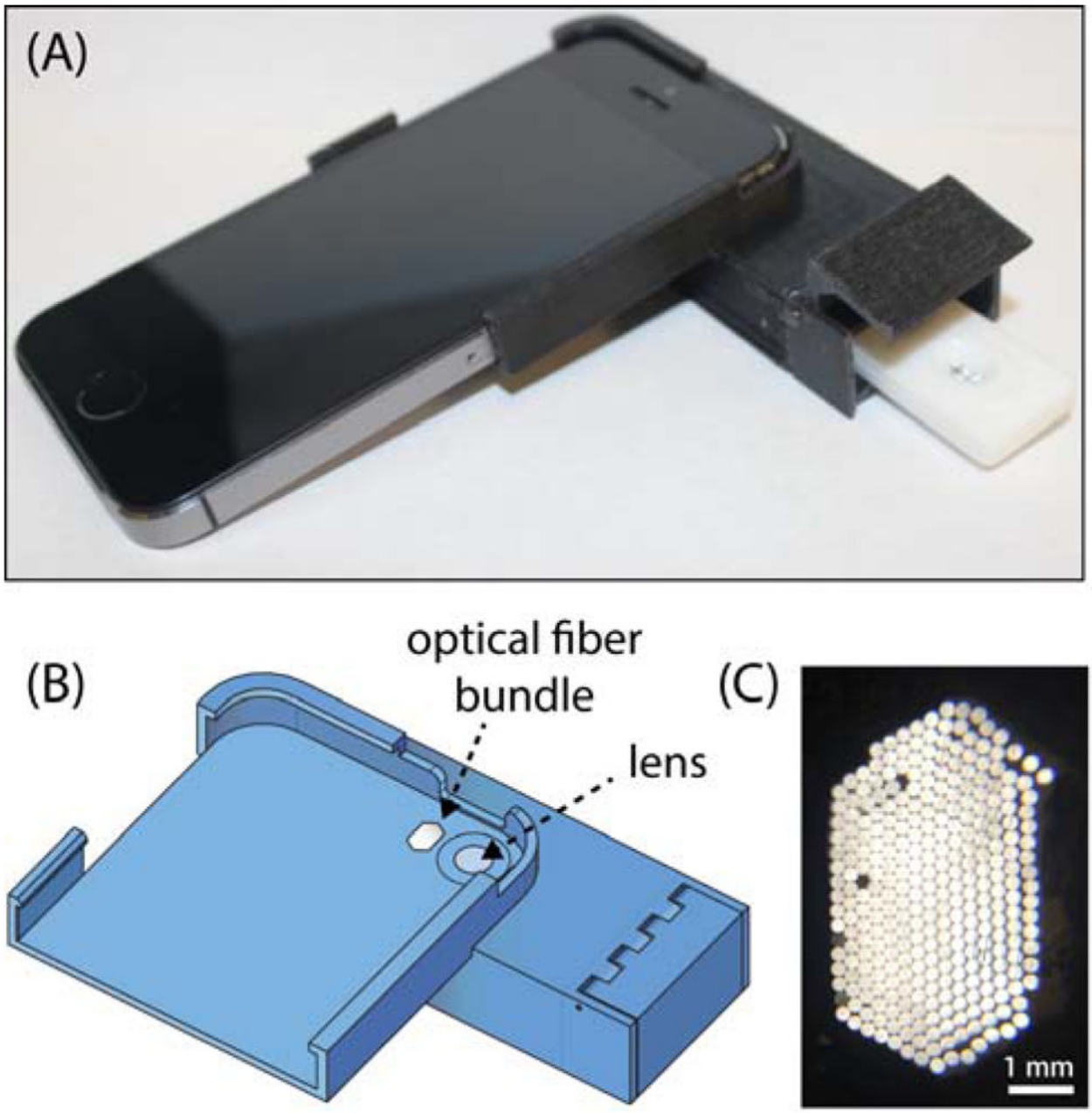

Figure 1.
(A) Image of smartphone attachment with LFA cartridge partially inserted. (B) CAD rendering of attachment noting the lens and optical fiber bundle. (C) Close-up image of optical fibers.

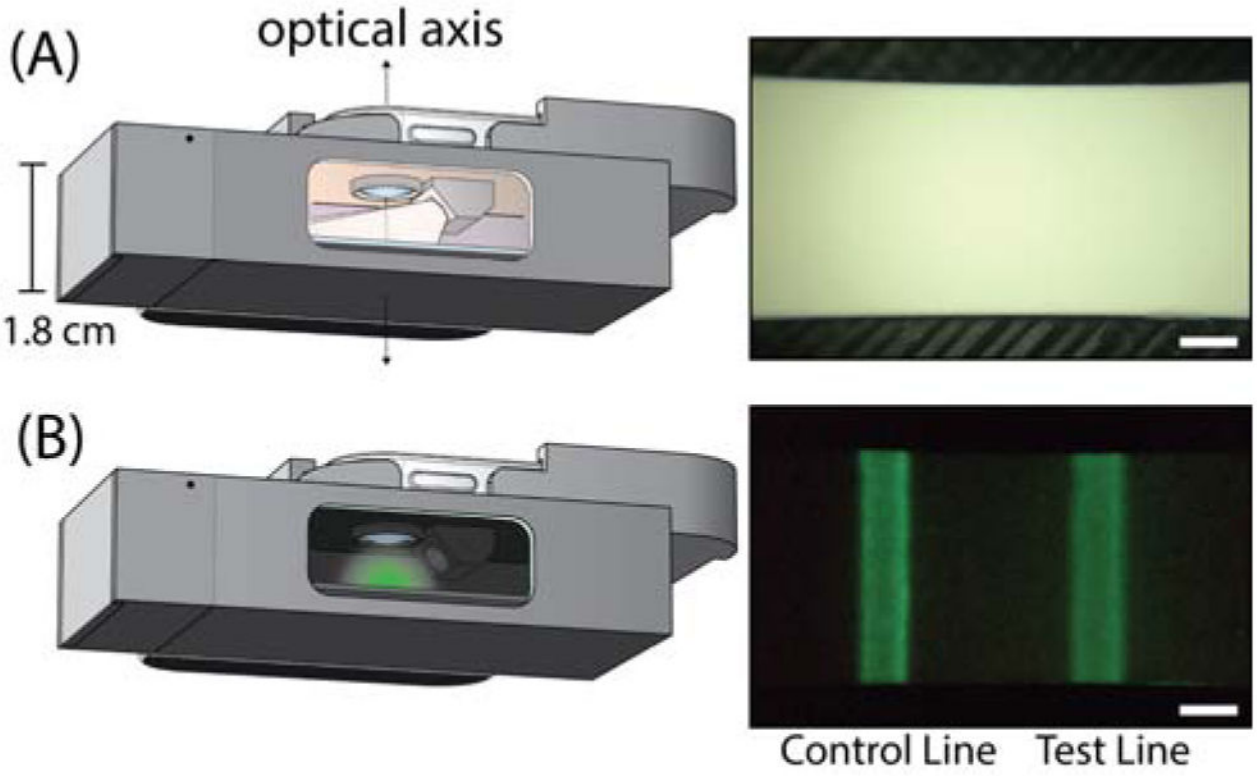

Figure 2.

Head-on view of the smartphone attachment on a phone with a cutaway to reveal the internal components and illustrate the time-gated imaging of an LFA strip (A) *Left*: phone's rear camera flash turned on for photoexcitation of phosphors. *Right*: image of the result window during excitation by phone's flash (B) *Left*: phone's flash turned off for luminescence imaging. *Right*: image of luminescence from anti-hCG persistent nanophosphors bound at the test line and control line of the strip at an hCG concentration of 0.12 ng/mL hCG (scale bar = 1 mm).

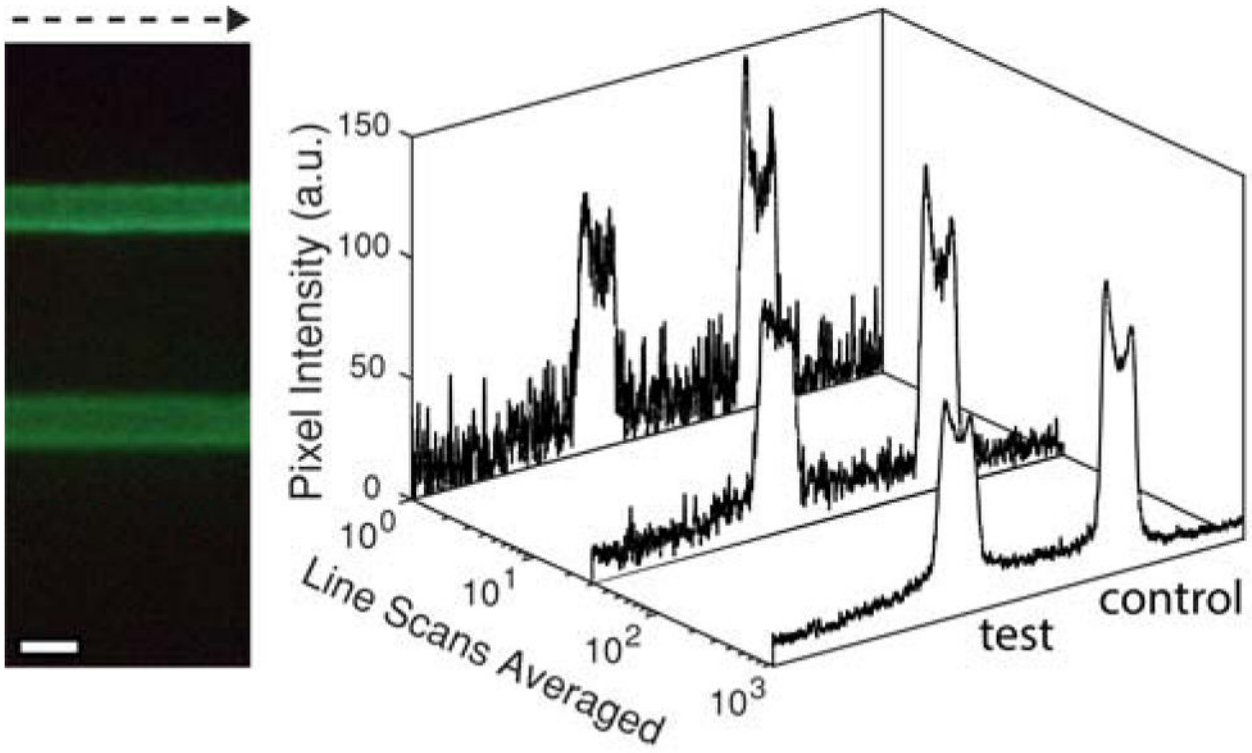

Figure 3.
Intensity profiles as a function of number of line scans averaged going from left to right across the width of a lateral flow strip ([hCG] = 0.12 ng/mL; scale bar = 1 mm).

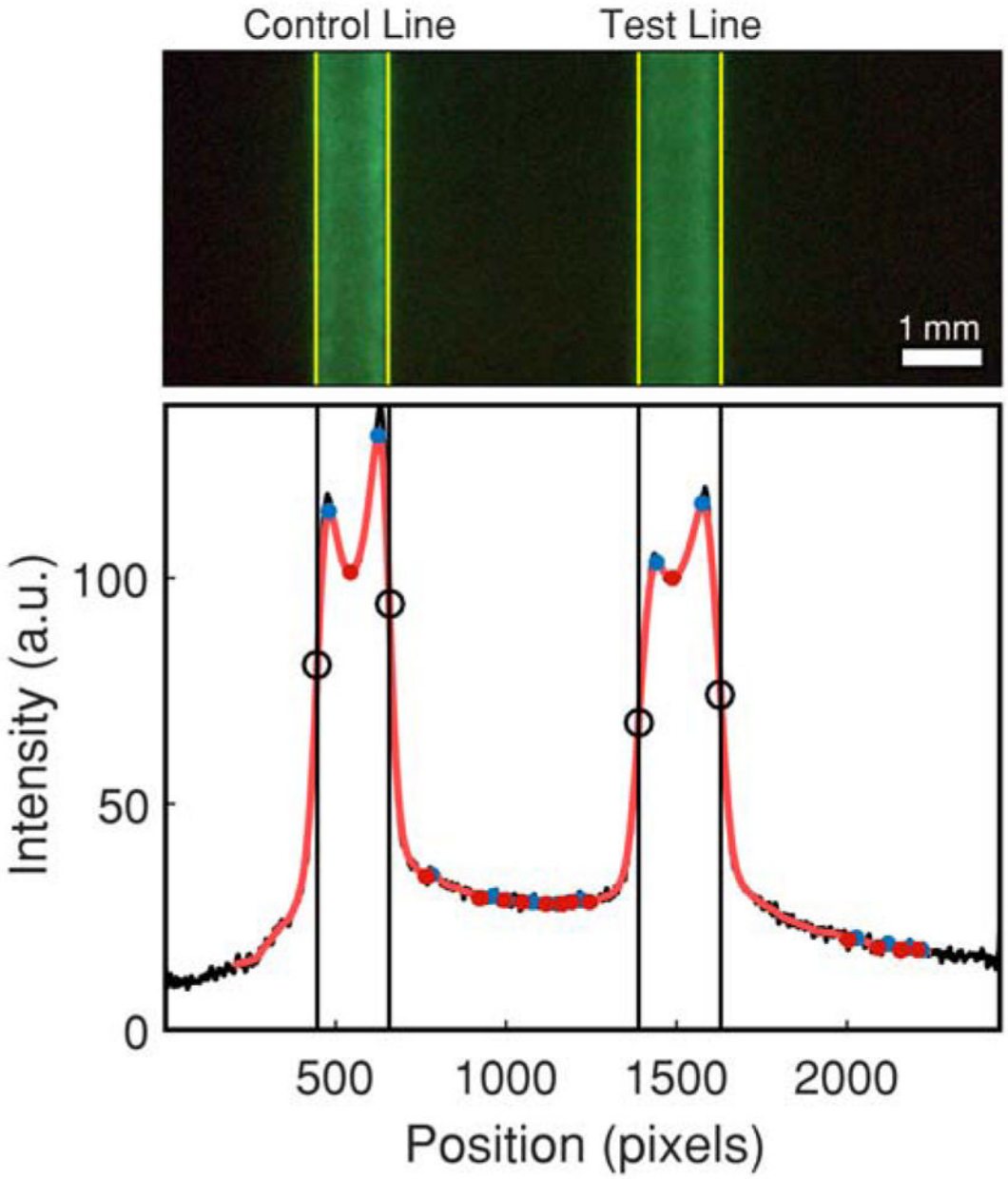

Figure 4.

Pixel averaging method for LFA strip run with 0.3 ng/mL hCG. Black circles denote inflection points which correspond to the edges of the test and control lines, which are marked by yellow lines on the image of the strip.

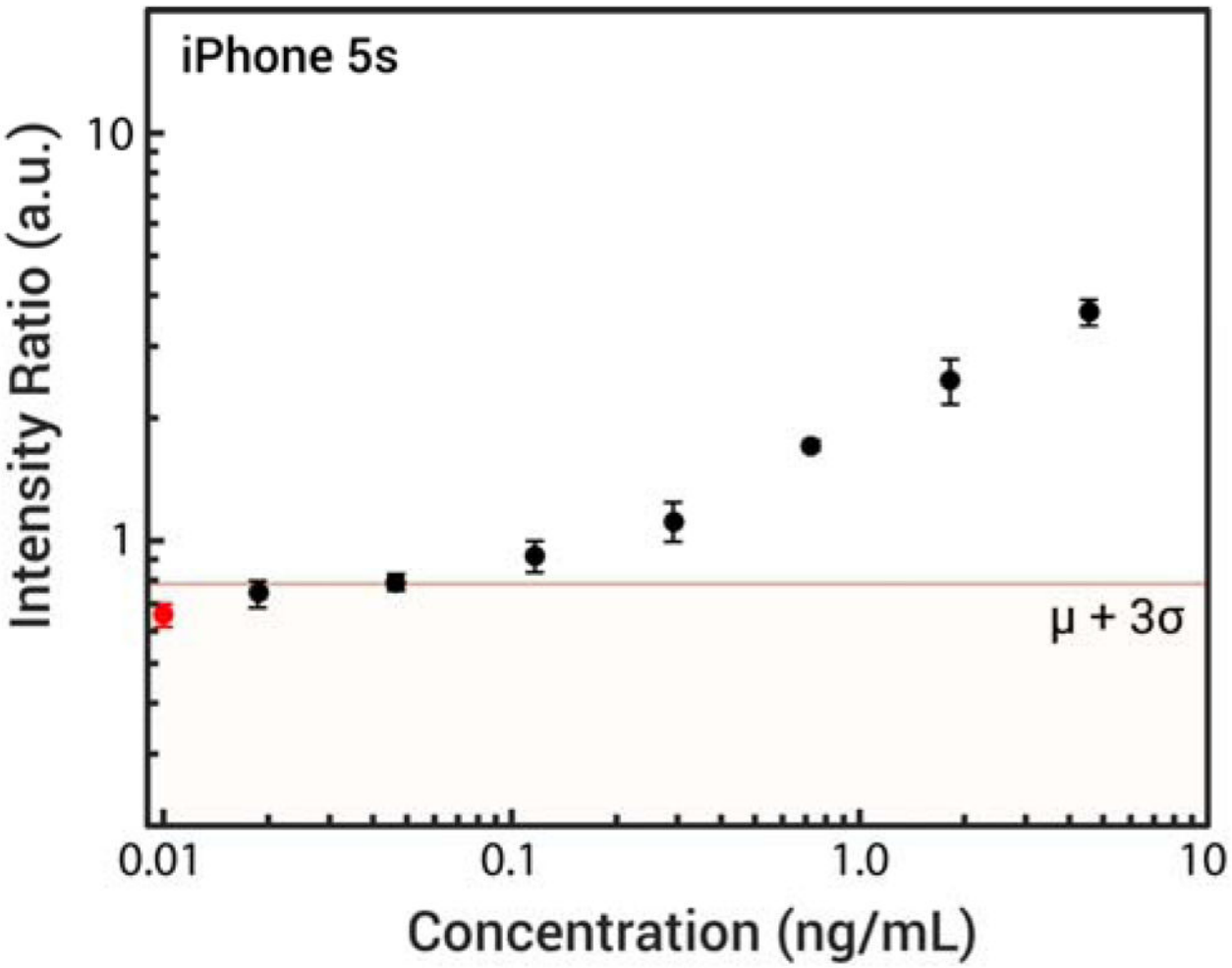

Figure 5.
Serial dilution of hCG detected with smartphone platform and strontium aluminate nanophosphors. The leftmost point on the plot, marked in red, corresponds to the mean and standard deviation of the blank samples. Horizontal line marks the mean of the blank plus three standard deviations.